Journal of the Physical Society of Japan
Vol. 78, No. 2, February, 2009, 023702
©2009 The Physical Society of Japan

Possible Superconductivity above 25 K in Single-Crystalline Co-Doped $BaFe_2As_2$

Yasuyuki NAKAJIMA[1,2*], Toshihiro TAEN[1], and Tsuyoshi TAMEGAI[1,2]

[1]*Department of Applied Physiscs, The University of Tokyo, 7-3-1 Hongo, Bunkyo-ku, Tokyo 113-8656*
[2]*JST, Transformative Research-Project on Iron Pnictides (TRIP), 7-3-1 Hongo, Bunkyo-ku, Tokyo 113-8656*

(Received November 17, 2008; accepted November 26, 2008; published January 26, 2009)

We present the superconducting properties of single-crystalline $Ba(Fe_{0.9}Co_{0.1})_2As_2$ by measuring its magnetization, resistivity, upper critical field, Hall coefficient, and magneto-optical images. The magnetization measurements reveal a fish-tail hysteresis loop at high temperatures and a relatively high critical current density above $J_c = 10^5$ A/cm^2 at low temperatures. The upper critical field determined by resistive transition is anisotropic with an anisotropic parameter of $\sim$3.5. Hall effect measurements indicate that $Ba(Fe_{0.9}Co_{0.1})_2As_2$ is a multiband system and that the mobility of electrons is dominant. Magneto-optical imaging reveals a prominent Bean-like penetration of vortices, although there is a slight inhomogeneity in a sample. Moreover, we observe distinct superconductivity above 25 K, which leads us to speculate that a higher transition temperature can be realized by fine-tuning the Co-doping level.

KEYWORDS: iron arsenide, magneto-optical imaging, critical current density, Hall coefficient, upper critical field
DOI: 10.1143/JPSJ.78.023702

Since the discovery of the high-T_c iron-based oxypnictide superconductor $LaFeAsO_{1-x}F_x$ with $T_c \sim 26$ K,[1] other iron-based superconductors have been sought for to obtain a higher transition temperature. In rare-earth-substituted iron oxypnictides RFeAsO$_{1-x}$F$_x$ (R = rare earth), transition temperature has been increased up to 55 K.[2] In these iron oxypnictides, superconductivity is induced by introducing electrons in the $(FeAs)^-$ layers by substituting F for O. Following these discoveries, oxygen-free iron-arsenide AFe$_2$As$_2$ (A = Ba, Sr, Ca) was discovered. These materials show superconductivity with the substitution of alkali metals, such as Na, K, and Cs, for A resulting in the introduction of holes in the $(FeAs)^-$ layers.[3–6] In hole-doped oxygen-free iron arsenides, transition temperature is increased to $\sim$38 K.[3,4] On the other hand, very recent studies revealed that the electron doping by the substitution of Co or Ni, which have one or two excess d electrons compared with Fe in conducting layers, induces superconductivity in oxygen-free iron arsenide.[7,8] In fact, nuclear magnetic resonance measurements have revealed that Co atoms donate electrons without generating localized moments.[9] Although the highest transition temperature in electron-doped $BaFe_2As_2$ is reported to be $\sim$23 K,[10] which is lower than that in hole-doped $BaFe_2As_2$, the fact that the substitution of transition metals leads to the induction of superconductivity contrasts strongly with a drastic suppression of T_c in cuprates.[11] However, detailed study of transition temperature as a function of Co-doping level is limited.[10] It is an open question whether the highest T_c in electron-doped $BaFe_2As_2$ can be increased further.

In this study, we prepare a single-crystalline sample of $Ba(Fe_{0.9}Co_{0.1})_2As_2$ and present its superconducting properties by studying its magnetization, resistivity, upper critical field, Hall coefficient, and magneto-optical images. We address the possibility of further enhancing transition temperature by fine-tuning Co-doping level.

Single-crystalline samples with a nominal composition of $Ba(Fe_{0.9}Co_{0.1})_2As_2$ were grown by the FeAs/CoAs self-flux method. FeAs and CoAs were prepared by placing mixtures of As pieces and Fe/Co powder in a silica tube and reacting them at 1065 °C for 10 h after heating at 700 °C for 6 h. A mixture with a ratio of Ba : FeAs : CoAs = 1 : 4.5 : 0.5 was placed in an alumina crucible with quartz fiber as a cup. The whole assembly was sealed in a large silica tube, and heated up to 1150 °C for 10 h followed by slow cooling down to 1090 °C at a rate of $\sim$1.3 °C/h, after which the silica tube was put in a centrifuge to separate crystals from flux. The typical size of the resulting crystals is $\sim 2 \times 2 \times 0.05$ mm^3. Magnetization was measured by a commercial SQUID magnetometer (Quantum Design MPMS-XL5). Resistivity measurement was performed by a four-contact method and Hall coefficient measurement was conducted using the standard six-wire configuration. Hall voltage was obtained from the antisymmetric part of transverse voltage by subtracting the positive and negative magnetic field data. Magneto-optical images were obtained using the local-field-dependent Faraday effect in an in-plane magnetized garnet indicator film and employing a differential method.[12,13]

Figure 1 shows the temperature dependence of zero-field-cooled (ZFC) and field-cooled (FC) magnetizations at 5 Oe along c-axis. A very sharp transition starting at $T_c \sim 24$ K is observed. It should be noted that T_c is the highest among those that have been reported to date.[7,9,10,14–17]

Figure 2(a) depicts the magnetization at several temperatures as a function of field. At high temperatures above 15 K, fish-tail magnetization is observed, which is very similar to that in $YBa_2Cu_3O_{7-\delta}$ single crystals.[18] From the magnetization hysteresis loop, we can obtain the critical current density J_c using the Bean model with the assumption of field-independent J_c. According to the Bean model, J_c is given by

$$J_c = 20 \frac{\Delta M}{a(1 - a/3b)}, \tag{1}$$

where ΔM is $M_{down} - M_{up}$, M_{up} and M_{down} are the magnetization when sweeping fields up and down, respectively, and a and b are the sample widths with $a < b$. Figure 2(b) shows the field dependence of J_c obtained from the data shown in Fig. 2(a) using eq. (1) and the effective sample dimensions with $a \sim 0.55$ mm and $b \sim 0.63$ mm. At low temperatures,

*E-mail: yasuyuki@ap.t.u-tokyo.ac.jp

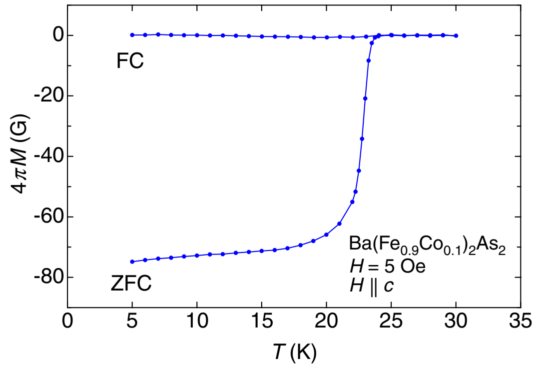

Fig. 1. (Color online) Temperature dependence of the zero-field-cooled (ZFC) and field-cooled (FC) magnetizations at $H = 5$ Oe along c-axis in Ba(Fe$_{0.9}$Co$_{0.1}$)$_2$As$_2$.

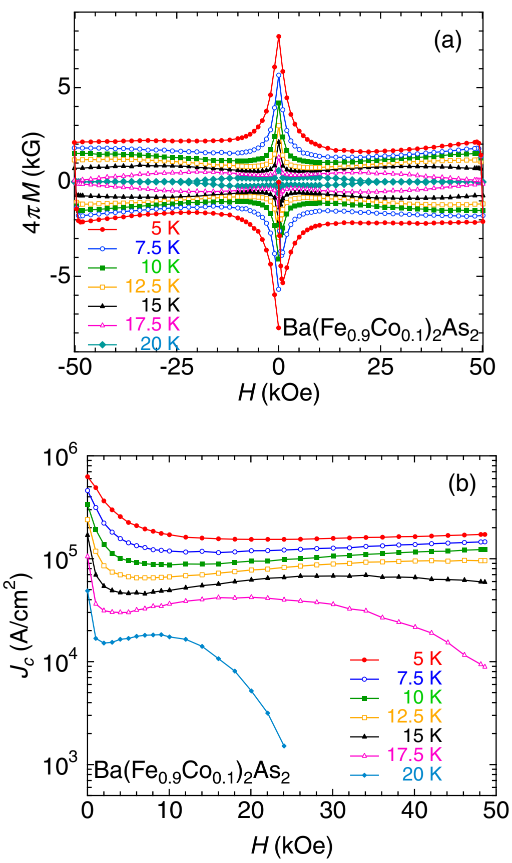

Fig. 2. (Color online) (a) Field dependence of magnetization in Ba(Fe$_{0.9}$Co$_{0.1}$)$_2$As$_2$ at 5, 7.5, 10, 12.5, 15, 17.5, and 20 K. (b) Field dependence of critical current density obtained from the data shown in Fig. 2(a) in Ba(Fe$_{0.9}$Co$_{0.1}$)$_2$As$_2$ at 5, 7.5, 10, 12.5, 15, 17.5, and 20 K.

J_c is larger than 10^5 A/cm^2. This value is much larger than that reported in ref. 7 and about twice as large as those reported in refs. 14 and 15. Although the present J_c is about one order of magnitude smaller than the typical value for YBa$_2$Cu$_3$O$_{7-\delta}$ single crystals,[19] it is well within the range for practical applications.

Figure 3(a) shows the temperature dependence of in-plane zero-field resistivity in Ba(Fe$_{0.9}$Co$_{0.1}$)$_2$As$_2$. With decreasing temperature from 300 K, resistivity decreases monotonically and then drops suddenly at T_c. There is no anomaly accompanied by a spin-density-wave transition reported in the parent material BaFe$_2$As$_2$,[20] which indicates that the

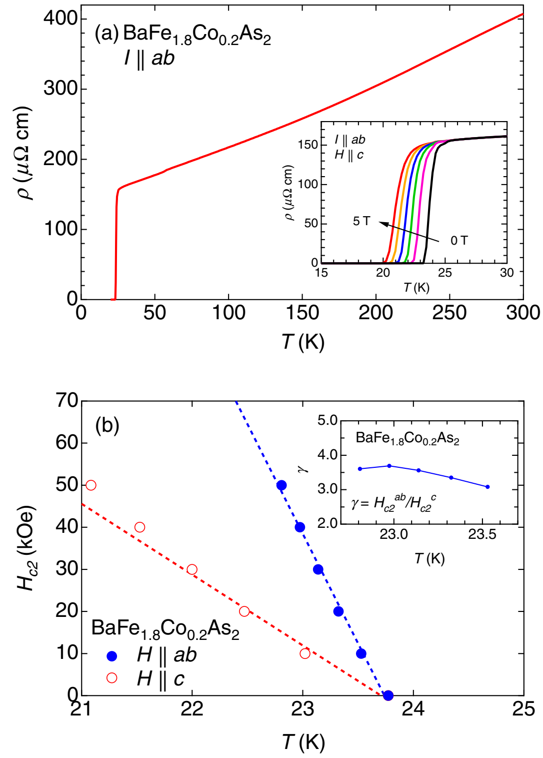

Fig. 3. (Color online) (a) Temperature dependence of zero-field resistivity in Ba(Fe$_{0.9}$Co$_{0.1}$)$_2$As$_2$. Inset: low-temperature in-plane resistivity data at $H = 0$, 10, 20, 30, 40, and 50 kOe along c-axis. (b) Temperature dependence of upper critical field along ab-plane (●) and c-axis (○) obtained using the midpoint of resistive transition in Ba(Fe$_{0.9}$Co$_{0.1}$)$_2$As$_2$. Dashed lines are linear fits to the data. Inset: temperature dependence of anisotropy of upper critical field along ab- and c-directions $\gamma \equiv H_{c2}^{ab}/H_{c2}^{c}$.

transition is suppressed by Co doping. The residual resistivity ratio $\rho(300\,\mathrm{K})/\rho(T_c)$ is $\sim$2.6, which is comparable to that reported before.[7,10,15,17] The inset of Fig. 3(a) depicts low-temperature in-plane resistivity data at $H = 0$, 10, 20, 30, 40, and 50 kOe along the c-axis. With increasing field, T_c decreases and transition width is broadened only slightly. We plot the upper critical field H_{c2} along the ab- and c-directions determined by the midpoint of resistive transition as a function of temperature in Fig. 3(b). The slopes of H_{c2} along the ab- and c-directions at T_c are -52.1 and -16.8 kOe/K, respectively. From the Werthamer–Helfand–Hohenberg theory,[21] which describes orbital depairing field of conventional dirty type-II superconductors, we can obtain the values of $H_{c2}(0) = 0.69T_c|dH_{c2}/dT|_{T=T_c} \sim 850$ and 280 kOe along the ab- and c-directions, respectively. These values are very high and comparable to that of hole-doped iron-arsenide superconductor Ba$_{1-x}$K$_x$Fe$_2$As$_2$.[22] The inset of Fig. 3(b) shows the anisotropy of the upper critical field $\gamma \equiv H_{c2}^{ab}/H_{c2}^{c}$. γ is $\sim$3–4 and slightly increases with decreasing temperature. This value is similar to that of hole-doped iron arsenide.[23]

Hall effect measurements strongly support that electrons are introduced by Co doping and that Ba(Fe$_{0.9}$Co$_{0.1}$)$_2$As$_2$ is a multiband system. Figure 4(a) shows the Hall resistivity ρ_{xy} at several temperatures as a function of field. In the present temperature region, ρ_{xy} is negative and shows an H-linear dependence. We plot the Hall coefficient R_H in Ba(Fe$_{0.9}$Co$_{0.1}$)$_2$As$_2$ obtained from ρ_{xy} as a function of temperature in Fig. 4(b). The sign of R_H is negative in the whole temper-

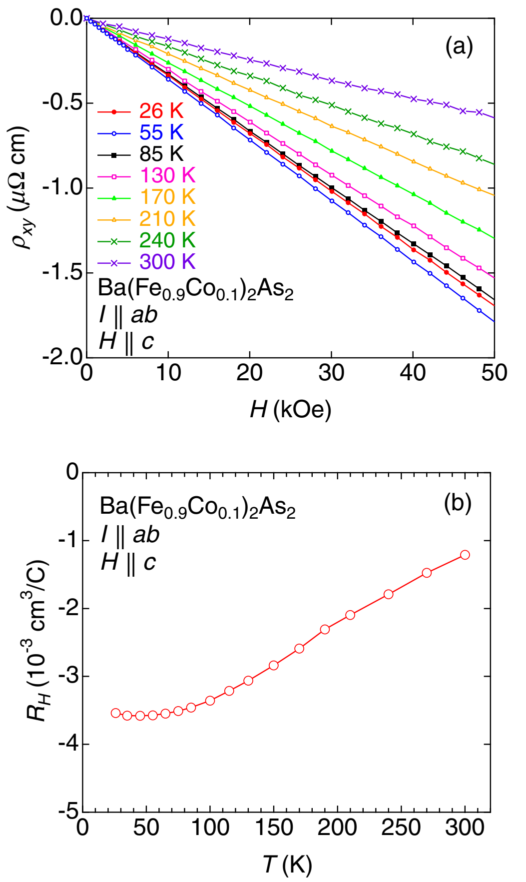

Fig. 4. (Color online) (a) Hall resistivity ρ_{xy} as a function of field at several temperatures. (b) Temperature dependence of the Hall coefficient in $Ba(Fe_{0.9}Co_{0.1})_2As_2$.

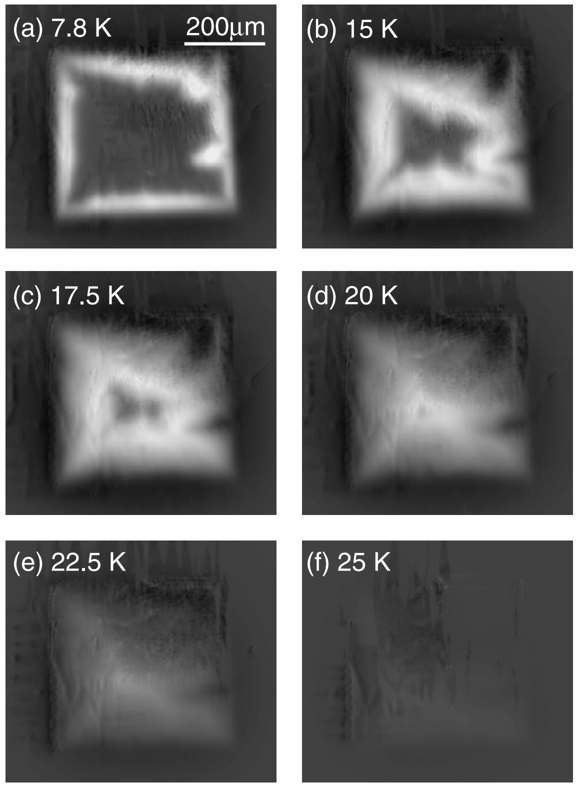

Fig. 5. Magneto-optical images of remanent state after applying $H = 690$ Oe in $Ba(Fe_{0.9}Co_{0.1})_2As_2$ at (a) 7.8, (b) 15, (c) 17.5, (d) 20, (e) 22.5, and (f) 25 K.

ature range, while that in the hole-doped $BaFe_2As_2$ is positive,[24] which is consistent with the introduction of electrons by Co substitution for Fe. R_H decreases with decreasing temperature from 300 to ~60 K and slightly increases after showing a broad minimum at ~50 K. The absolute value of R_H just above T_c is three times larger than that at 300 K. In a simple single-band system without strong spin fluctuations, the Hall coefficient is written as, $R_H = 1/nq$, where q is the charge of a carrier and n is the carrier density. R_H is almost T-independent. By contrast, the Hall coefficient in a multiband system, for instance, consisting of electron and hole bands, is given by $R_H = (n_h\mu_h^2 - n_e\mu_e^2)/[e(n_h\mu_h + n_e\mu_e)^2]$, where n_h (n_e) is the density of holes (electrons) and μ_h (μ_e) is the mobility of holes (electrons). The Hall coefficient in a multiband system can be temperature-dependent. The obtained results indicate that $Ba(Fe_{0.9}Co_{0.1})_2As_2$ is a multiband system similar to the parent material $BaFe_2As_2$[25] and mobility of the electrons produced by Co doping becomes dominant with decreasing temperature.

Figure 5 shows magneto-optical images of $Ba(Fe_{0.9}Co_{0.1})_2As_2$ in the remanent state at several temperatures after cycling the field up to 690 Oe for 5 s. Although the sample for the magneto-optical experiment is different ($0.58 \times 0.45 \times 0.03$ mm^3) from that for the magnetization measurement, both crystals show similar properties. The bright region in the figures corresponds to the area trapping the vortices. Dark faint zig-zag features originate from in-plane domains of the garnet film and have nothing to do with the flux distribution. At lower temperatures, vortices that penetrated from the edges of the crystal cannot reach the center owing to the large shielding current. However, prominent penetrations of vortices are observed near the defects close to the right edge of the sample. The penetration of vortices develops with increasing temperature. It should be noted that the image at 25 K apparently shows existence of superconductivity in the lower part of the sample. In fact, zero-field resistivity starts to drop at ~25 K, as shown in the inset of Fig. 3(a). The highest transition temperature in $Ba(Fe_{1-x}Co_x)_2As_2$ reported so far is ~23 K.[10] The difference can originate from the difference in Co concentration and/or its distribution. It may be possible to obtain an even higher transition temperature in this system by fine-tuning the Co doping level.

In summary, we have presented a systematic study of magnetization, resistivity, upper critical field, Hall coefficient, and magneto-optical imaging in single-crystalline $Ba(Fe_{0.9}Co_{0.1})_2As_2$. The magnetization measurements reveal a fish-tail hysteresis loop at high temperatures and a relatively high critical current density larger than 10^5 A/cm^2. The upper critical field obtained by resistive transition is anisotropic and its anisotropy is about 3.5. Hall effect measurements indicate that $Ba(Fe_{0.9}Co_{0.1})_2As_2$ is a multiband system and the mobility of electrons is dominant. The magneto-optical imaging reveals prominent Bean-like penetrations of vortices although there is slight inhomogeneity in a sample. We also find distinct superconductivity above 25 K, which leads us to expect that a higher transition temperature can be realized by fine-tuning Co-doping level.

1) Y. Kamihara, T. Watanabe, M. Hirano, and H. Hosono: J. Am. Chem. Soc. **130** (2008) 3296.
2) Z. A. Ren, W. Lu, J. Yang, W. Yi, X. L. Shen, Z. C. Li, G. C. Che, X. L. Dong, L. L. Sun, F. Zhou, and Z. X. Zhao: Chin. Phys. Lett. **25** (2008) 2215.
3) M. Rotter, M. Tegel, and D. Johrendt: Phys. Rev. Lett. **101** (2008) 107006.
4) G. F. Chen, Z. Li, G. Li, W. Z. Hu, J. Dong, X. D. Zhang, P. Zheng, N. L. Wang, and J. L. Luo: Chin. Phys. Lett. **25** (2008) 3403.
5) K. Sasmal, B. Lv, B. Lorenz, A. Guloy, F. Chen, Y. Xue, and C. W. Chu: Phys. Rev. Lett. **101** (2008) 107007.
6) G. Wu, H. Chen, T. Wu, Y. L. Xie, Y. J. Yan, R. H. Liu, X. F. Wang, J. J. Ying, and X. H. Chen: J. Phys.: Condens. Matter **20** (2008) 422201.
7) A. S. Sefat, R. Jin, M. A. McGuire, B. C. Sales, D. J. Singh, and D. Mandrus: Phys. Rev. Lett. **101** (2008) 117004.
8) L. J. Li, Q. B. Wang, Y. K. Luo, H. Chen, Q. Tao, Y. K. Li, X. Lin, M. He, Z. W. Zhu, G. H. Cao, and Z. A. Xu: arXiv:0809.2009.
9) F. L. Ning, K. Ahilan, T. Imai, A. S. Sefat, R. Jin, M. A. McGuire, B. C. Sales, and D. Mandrus: J. Phys. Soc. Jpn. **77** (2008) 103705.
10) N. Ni, M. E. Tillman, J.-Q. Yan, A. Kracher, S. T. Hannahs, S. L. Bud'ko, and P. C. Canfield: arXiv:0811.1767.
11) H. Fujishita and M. Sato: Solid State Commun. **72** (1989) 529.
12) A. Soibel, E. Zeldov, M. Rappaport, Y. Myasoedov, T. Tamegai, S. Ooi, M. Konczykowski, and V. B. Geshkenbein: Nature **406** (2000) 282.
13) M. Yasugaki, K. Itaka, M. Tokunaga, M. Kameda, and T. Tamegai: Phys. Rev. B **65** (2002) 212502.
14) A. Yamamoto, J. Jaroszynski, C. Tarantini, L. Balicas, J. Jiang, A. Gurevich, D. C. Larbalestier, R. Jin, A. S. Sefat, M. A. McGuire, B. C. Sales, D. K. Christen, and D. Mandrus: arXiv:0810.0699.
15) R. Prozorov, N. Ni, M. A. Tanatar, V. G. Kogan, R. T. Gordon, C. Martin, E. C. Blomberg, P. Prommapan, J. Q. Yan, S. L. Bud'ko, and P. C. Canfield: arXiv:0810.1338.
16) R. T. Gordon, N. Ni, C. Martin, M. A. Tanatar, M. D. Vannette, H. Kim, G. Samolyuk, J. Schmalian, S. Nandi, A. Kreyssig, A. I. Goldman, J. Q. Yan, S. L. Bud'ko, P. C. Canfield, and R. Prozorov: arXiv:0810.2295.
17) F. Ning, K. Ahilan, T. Imai, A. S. Sefat, R. Jin, M. A. McGuire, B. C. Sales, and D. Mandrus: J. Phys. Soc. Jpn. **77** (2008) 103705.
18) M. Däumling, J. M. Seuntjens, and D. C. Larbalestier: Nature **346** (1990) 332.
19) T. Tamegai, L. Krusin-Elbaum, L. Civale, P. Santhanam, M. J. Brady, W. T. Masselink, F. Holtzberg, and C. Feild: Phys. Rev. B **45** (1992) 8201.
20) M. Rotter, M. Tegel, D. Johrendt, I. Schellenberg, W. Hermes, and R. Pöttgen: Phys. Rev. B **78** (2008) 020503R.
21) N. R. Werthamer, E. Helfand, and P. C. Hohenberg: Phys. Rev. **147** (1966) 295.
22) M. Altarawneh, K. Collar, C. H. Mielke, N. Ni, S. L. Bud'ko, and P. C. Canfield: arXiv:0807.4488.
23) N. Ni, S. L. Bud'ko, A. Kreyssig, S. Nandi, G. E. Rustan, A. I. Goldman, S. Gupta, J. D. Corbett, A. Kracher, and P. C. Canfield: Phys. Rev. B **78** (2008) 014507.
24) G. Wu, R. H. Liu, H. Chen, Y. J. Yan, T. Wu, Y. L. Xie, J. J. Ying, X. F. Wang, D. F. Fang, and X. H. Chen: Europhys. Lett. **84** (2008) 27010.
25) C. Liu, G. D. Samolyuk, Y. Lee, N. Ni, T. Kondo, A. F. Santander-Syro, S. L. Bud'ko, J. L. McChesney, E. Rotenberg, T. Valla, A. V. Fedorov, P. C. Canfield, B. N. Harmon, and A. Kaminski: Phys. Rev. Lett. **101** (2008) 177005.